

1 **Title page**

2 **Morphological Alternations of Intraepithelial and Stromal Telocytes in Response to**
3 **Salinity Challenges**

4

5 *The full names of all authors.*

6 **Soha Mohamed Abdel-latif Soliman (corresponding author)**

7 lecturer of Histology

8 Department of Histology

9 Faculty of Veterinary Medicine, South Valley university, Qena, Egypt.

10 Postal code. 83523. Tel. +201006500848. Fax. +2 09652112231627. Email.

11 Soha.soliman@yahoo.com

12 soha_soliman@vet.svu.edu.eg

13

14 **Walaa Fathy Ali Emeish**

15 lecturer of fish Diseases

16 Department of fish Diseases

17 Faculty of Veterinary Medicine, South Valley university, Qena 83523, Egypt.

18 walaavet2002@yahoo.com

19

20

21

22 **The current study was carried out in South Valley University**

23

24

25

26 *Short title telocytes responding to salinity*

27

28 **Keywords** intraepithelial telocytes, stromal telocytes, salinity, chloride cells, stem cells,

29 Rodlet cells.

30

31 ***Summary statement***

32 The article represent an experimental study in which we investigated the effect of the
33 ssalinty on the communicating cells (telocytes) and their target cells including chloride,
34 stem, Rodlet cells, myoblasts
35

36 **Morphological Alternations of Intraepithelial and Stromal**
37 **Telocytes in Response to Salinity Challenges**

38

39 **Soha A. Soliman¹, Walaa F.A. Emeish²**

40

41

42 ¹ Department of Histology, Faculty of Veterinary Medicine, South Valley University, Qena 83523, Egypt. (e-mail,
43 (soha.soliman@yahoo.com)

44 ² Department of fish Diseases Faculty of Veterinary Medicine, South Valley university, Qena 83523, Egypt.(e-mail,
45 walaavet2002@yahoo.com).

46

47 **Abstract**

48 Telocyte is a communicating cell established relations to various types of cells.
49 Few experimental studies are performed on telocytes. The current study investigated
50 response of telocytes to salinity stress in relations to osmoregulatory, immune and stem
51 cells. We exposed Common carp to salinity level 0.2, 6, 10, 14 ppt. Gill samples were
52 fixed and processed for microscopic and TEM. Two types of telocytes were identified:
53 intraepithelial and stromal telocytes. Intraepithelial telocytes comprised the cellular lining
54 of the lymph spaces where they shed the secretory vesicles. Stromal telocytes shed their
55 secretory vesicles in the secondary circulatory vessels. Telocyte enlarged and exhibited
56 high secretory activities. They exert their effect either by direct contact or by paracrine
57 mode. In salinity treated samples, chloride cells enlarged and the mitochondria became
58 cigar-shaped. pavement cells enlarged and micro-ridges elongated. Stromal telocytes
59 established contact with stem cell and skeletal myoblast. Macrophages and Rodlet cells
60 increased in number. In conclusion, intraepithelial and stromal responded to salinity
61 stress by activation of cellular signaling. They play a major role in osmoregulation,
62 immunity, and regeneration.

63

64 **Keywords** intraepithelial telocytes, stromal telocytes, salinity, chloride cells, stem cells,
65 Rodlet cells.

66

67 **introduction**

68 Telocyte is a distinctive type of interstitial cells, which have a wide range of
69 biological functions in different tissues and organs. Functional diversity of telocytes is
70 regarding affecting different types of cells and structures (**Varga, Danisovic et al. 2016**).
71 Telocytes have unique morphological characteristics. Multiple cell prolongations;
72 telopodes emerge from the cell body and may extend to hundreds of microns. Telopodes
73 may give rise dichotomous branches and establish cellular connections to form a complex
74 labyrinthine system. Telopodes composed of thin segments; podomers and interval
75 expansions; podoms which are rich in calcium release units; mitochondria, endoplasmic
76 reticulum, and caveolae. Telocytes establish a synaptic junction connecting to
77 immunoreactive cells (**Popescu and Fausone-Pellegrini 2010**).

78

79 Telocytes exert their effect on cells either by establishing cellular contact or
80 through paracrine mode. Two types of cellular contact are documented for telocytes;
81 homocellular and heterocellular contact. Homocellular contact is formed between two
82 telopodes or telocytes and telopodes or between the cell body of two adjacent telocytes.
83 Heterocellular type contact between telocytes and stromal cells either fixed or the free
84 cells. Various types of cellular contacts and communication are mentioned in telocytes
85 including direct apposition of the cell membrane of adjacent telocytes, adherence, and

86 gap junction. Gap junction have a significant role in intercellular signaling pathway
87 (**Mirancea 2016**). The secretory function of telocytes influence the target cells.
88 Telocytes deliver microvesicles to the cell and providing macromolecules such as
89 proteins or RNAs, microRNA. Telocytes also shed exosomes, ectosomes and
90 multivesicular vesicles (**Popescu, Gherghiceanu et al. 2005; Popescu and Fausone-**
91 **Pellegrini 2010; Cantarero Carmona, Luesma Bartolome et al. 2011**)

92

93 Telocytes are multifunctional cell functions. They contribute to generation and
94 transmission of nerve impulses to involuntary muscles (**Takaki 2003; Hutchings,**
95 **Williams et al. 2009; Gandahi, Chen et al. 2012; Drumm, Koh et al. 2014**). They
96 serve in mechanoreception and may involve in atrial fibrillation (**Gherghiceanu,**
97 **Hinescu et al. 2008**). Telocytes exhibit receptors for excitatory and inhibitory
98 neurotransmitters (**Iino and Horiguchi 2006**). They establish contact with
99 immunoreactive cells such as eosinophil (**Cantarero Carmona, Luesma Bartolome et**
100 **al. 2011**), mast cell, and macrophage (**Gherghiceanu and Popescu 2012**). Telocytes
101 play a role in regeneration of heart, lung, skeletal muscle, skin, meninges and choroid
102 plexus, eye, liver, uterus, urinary system (**Bei, Wang et al. 2015**).

103

104 Several studies are conducted to study telocytes in human and other mammals but
105 few studies are performed in aquatic species. the current study was conducted using the
106 common carp. The carp belong to *Cyprinidae* family which is commonly known in North
107 America as minnow, while in Eurasia is termed as carp. *Cyprinidae* family are freshwater

108 and are uncommon in brackish water; North America, Africa, and Eurasia (**Nelson**
109 **2006**).

110

111 Aquatic species regulate ionic exchange to maintain osmotic balance according to
112 environmental salinity. Several organs are involved in osmoregulation including gills,
113 intestine, kidney, skin, operculum (**Marshall and Grosell 2005**). Marine inhabitants face
114 great challenges to establish ionic balance. Therefore, the ion transporting cells; chloride
115 cells or ionocytes; participate in the elimination of excess ions in seawater fish, while in
116 freshwater fish, chloride cells contribute in ion absorption (**Florkin 2014**). IN MARINE
117 FISH, Chloride cells are structurally modified to adopt high salinity levels. Fish exposed
118 to high salinity environment acquire a high proportion of mitochondrial-rich chloride
119 cells (**Fielder, Allan et al. 2007**). Pervious researches studied the salinity in relation to
120 changes of ionocytes cells. Ionocytes serve in osmoregulation via different types of
121 membranous channels; cystic fibrosis transmembrane regulator (CFTR) anion channel,
122 Na,K,2Cl cotransporter (NKCC) and sodium pump (Na,K-ATPase). CFTR is considered
123 as a membrane protein located on the apical surface of many types of epithelial cells.
124 CFTR is a cyclic AMP-dependent chloride channel, a bicarbonate channel and as a
125 modulator of other ion channels (**Derichs 2013**). The Na-K-Cl cotransporter (NKCC) is a
126 membrane transport proteins that involved in the active transport of sodium, potassium,
127 and chloride ions across the cell membrane (**Russell 2000**). Na-K-ATPase is an
128 electrogenic transmembrane enzyme located predominantly on the basolateral surface of
129 the chloride cell and actively transport chloride, rather than sodium across the plasma
130 membrane (**Suhail 2010**). Pavement cells mostly cover the surface the of the filament and

131 lamellar epithelium. They considered as ion transporting cells; their cell membrane is rich
132 in hydrogen ion channels (**Laurent, Goss et al. 1994; Perry and Fryer 1997**). In the
133 current study, we focused on the communicating cells; telocytes which influence the
134 large population of stromal, muscular, and epithelial cells. The aim of the present study
135 was to investigate morphological alternations of telocytes subjected to salinity stress and
136 their effect on different types of cells with special reference to the osmoregulatory and
137 immune and stem cells in the common carp.

138

139

140 **Materials and methods**

141 **I- Fish source and transportation**

142 The common carp, *Cyprinus carpio*. was obtained from a private fish farm at El-
143 Dakahlea Government and transported in large water tanks. During transportation, the
144 oxygen level was maintained at 5 mg/l and water tank temperature was 23°C ±3 and pH
145 value at 7.2 – 7.5.

146 **II- Fish acclimation**

147 Apparently, healthy fingerlings fish measured about the length of 7±2 cm and aged 1
148 month old. The body weight was 10±2 g, and. Fish were collected and transported to the
149 wet laboratory at Faculty of Veterinary Medicine, South Valley University, Qena, Egypt.
150 Fish were maintained under laboratory conditions during adaptation in running water
151 (salinity = 0.2 ppt) for 3 weeks before conducting the experiments and fed twice daily to
152 ad libitum feed on a commercial floating powdered feed containing 45% protein with a
153 feeding rate of 3% of their body weight.

154

155 **III- Aquaria**

156 Fish were originally kept in a re-circulating system in porcelain aquaria (260 ×65×70cm)
157 according to the protocol of maintaining bioassay fish as was previously described
158 (Ellsaesser and Clem, 1986). Experiments were conducted in fiberglass aquaria with
159 dimensions of 60×30×40 cm. Dissolved oxygen level was maintained above 5 mg/l while
160 water temperature was kept at 23°C ±3 and pH value at 7.2 – 7.5.

161

162 **IV- Salinity exposure**

163 36 acclimated, apparently healthy Common carp, *C. carpio* were selected with a body
164 weight range of 9 – 11 g to serve as the experimental groups. Fish were divided into 12
165 fiberglass aquaria (60×30×40 Cm) to serve as 4 experimental groups, each group contains
166 9 fish, and there were 3 replicates for each salinity group. Three groups were gradually
167 subjected to three different salinities until concentrations of 6, 10 and 14 ppt with 2 g/L
168 NaCl increase every two days. The fourth group was reared in freshwater; a dechlorinated
169 tap water of 0.2 ppt salinity level and considered as control group. Water was changed
170 every two days with water that had desired salinities, and aquariums were also cleaned at
171 this time. Salinity was checked and adjusted regularly every two days during a water
172 change. When common carp reached the final desired salinity, fish were allowed to
173 acclimate to the new salinities for a minimum of two weeks before sample collections.

174

175 **V- Clinical examination of fish**

176 Fish were observed daily during the course of an experiment for any apparent clinical
177 signs, lesions or mortality. Mortality rate was calculated from the number of dead fish
178 between each sampling period.

179

180 **VI- Fish sampling**

181 At the end of the period, nine fish were decapitated in each salinity level. Gill filaments
182 and gill arches of both sides were dissected and fixed in glutaraldehyde (10 mL of 2.5%
183 glutaraldehyde and 90 mL 0.1 M Na-phosphate buffered formalin).

184

185 **VII- preparation of resin embedding specimens for semi-thin and ultra-thin** 186 **sectioning**

187 Fixed samples of gill filaments and arches were cut into small pieces. They were washed
188 4 times for 15 minutes in 0.1 M sodium phosphate buffer (pH 7.2) then were post-fixed in
189 1% osmic acid in 0.1 M Na-phosphate buffer at 4°C for 2 hours. The osmicated samples
190 were washed 3 times for 20 minutes in 0.1 M phosphate buffer (pH 7.2). Dehydration
191 was performed through graded acetone (70, 80, 90, 100%), 10 minutes for each
192 concentration. The dehydrated samples were immersed in a mixture of acetone/resin (1/1
193 for 1day, ½ for another day) and pure resin for three days. The resin was prepared by
194 using 10gm ERL, 6gm DER, 26gm NSA and 0.3gm DMAE and thoroughly mixed by a
195 shaker. The specimens were embedded in the resin at 60 C° for 3 days. Polymerized
196 samples were cut to semi-thin sections by using an ultramicrotome Ultracut E (Reichert-
197 Leica, Germany) and stained with toluidine blue (**Bancroft, Layton et al. 2013**).

198

199 Semi-thin sections were also used in histochemical studies. The sections were treated
200 with a saturated alcoholic solution of sodium hydroxide for 15 minutes to dissolve the
201 resin (**Lloyd 2001**). The semi-thin sections were stained by Heidenhain's Iron-Hx
202 (**Heidenhai 1896**) and methylene blue used for staining of paraffin sections and prepared
203 as a stain for semi-thin sections (**Bancroft, Layton et al. 2013**).

204

205 Ultrathin sections were obtained by a Reichert ultra-microtome. The sections (70 nm)
206 were stained with uranyle acetate and lead citrate (Reynolds, 1963) and examined by
207 JEOL100CX II transmission electron microscope (TEM) at the CENTREAL
208 LABARTORY UNIT of South Valley University.

209

210 **VIII- Coloring images**

211 Transmission electron microscopy images were colored using photo filter 6.3.2
212 program. Coloring images required to change the color balance, using the stamp tool to
213 color the objective cells.

214

215 **Results**

216

217 The current study was performed to evaluate ranges of acclimation of the
218 common carp to the hypertonic conditions in relation to responses of the communicating
219 cells; telocytes and the related effector cells including immune, chloride and stem cells in
220 gill filaments and arches using semi-thin and ultrathin sections.

221

222 Control and 6ppt salinity exposed groups exhibited normal morphology and behavior and
223 had no noticeable signs of stress and no mortality. However, marked reduction of
224 swimming speed and fish were easily caught in 10 and 14 ppt salinity treated fish.

225

226 By semi-thin sections, intraepithelial telocytes had a small cell body and well-defenind
227 telopodes in control samples (Fig. 1A, E, I). They were gradually enlarged in size during
228 exposure to different levels of salinity. In 6 ppt, intraepithelial telocytes were satellite in
229 shape (Fig. 1B, F, J). In 10 ppt and 14 ppt they were large satellite cells with multiple
230 telopodes Fig. 1C, D, G, H, K, L). stromal telocytes were small and had spindle-shaped
231 cell body form which extended fine telopodes in control samples (Fig. 2A, E, I). In 6 ppt
232 salinity concentration, some stromal telocytes were enlarged and telopodes formed a
233 network (Fig. 2 B, F, J). Telopodes formed an extensive network; secretory vesicles were
234 large and could be easily recognized in samples treated with 10 and 14 ppt salinity levels
235 (Fig 2 C, D, G, H, K, L).

236

237 Telocytes were identified for the first time by TEM in the epithelium of the gill arches. In
238 control samples, telocytes represented the cellular lining of the intraepithelial lymphatic
239 space in which immuno-reactive cells migrate. Intraepithelial telocytes were small, had
240 spindle or satellite-shaped, their telopodes were thin and formed a labyrinth network
241 separating between the compartments of the lymphatic space. Intraepithelial telocytes rest
242 on the basement membrane. Telopodes extended between epithelial and immune cells.
243 Intraepithelial telocytes could establish contact with epithelial cells. The secretory
244 vesicles of the telopodes were excreted in the intraepithelial lymphatic space (Fig 4 A,

245 B). In samples treated with 60 ppt salinity level, intraepithelial telocytes undergo
246 hypertrophy and telopodes were thickened (Fig. 4 C-H).

247

248 In 10 salinity concentration, intraepithelial telocytes was hypertrophy associated with
249 enlargement of the podoms. They also acquired high secretory activity. Intraepithelial
250 telocytes established planar contact with chloride cell (Fig 5A-E). In 14 ppt salinity
251 level, telocytes shed secretory vesicles, exosomes, and multivesicular vesicle into the
252 intra-epithelial lymphatic spaces. Intra-epithelial telocytes established planar contact with
253 chloride cells (Fig 6A- D).

254

255 Stromal telocytes appeared small spindle, satellite, rounded, triangular shaped cell body
256 with thin cellular prolongations (telopodes) in control samples. Telopodes consisted of
257 podoms and podomers. Macrophages were small and contained vesicles (Fig. 7 A, B, Fig.
258 8A, B). Telocytes established homocellular junction (Fig 7 C, D). Stromal telocytes
259 undergo morphologically modifications during increasing the concentration of the
260 salinity. The cell body of some populations of telocytes enlarged in salinity levels of 6
261 ppt (Fig 4 C-H), and 10 ppt (Fig. 5 A, F). In 10 ppt salinity level, telopodes were
262 thickened and became slightly wavy (Fig. 7E, F). Telopodes frequently formed an
263 extensive network (Fig. 8 F). The prominent features of high salinity changes were
264 irregular surface telocyte, waviness, and thickening of telopodes (Fig 7 G, H). They
265 exhibited higher secretory activities in salinity levels reached 6, 10, and 14 ppt (Fig 8 A-
266 D). Stromal telocytes established contact with the endothelial lining of the secondary
267 circulatory system or lymph vessels and liberated the secretory vesicles in proximity to

268 the vessels. Trans-endothelial transportation of the secretory vesicles was observed in the
269 secondary circulatory vessels. The transferring vesicles were shed in the lumen of the
270 secondary circulatory pathway (Fig. 4G, Fig. 6E, Fig. 8E, F).

271

272 Telocytes established contact with different types of stromal, epithelial, stem cells and
273 skeletal muscles. Telopodes were connected to nerve fiber (Fig 12A-C) and formed point
274 contact (fig. 7B) or multipoint contact (Fig 12A-C) with skeletal muscles. Large amount
275 of secretory vesicles were excreted closed to the muscular fibers in samples treated with 6
276 ppt concentration of salinity (Fig 12A, C). An extensive network of telopodes was
277 observed and more secretory vesicles were shed form telocytes. Skeletal muscle fiber
278 undergoes hypertrophy after reaching 10 ppt salinity concentration (Fig. 12D, E).

279 Both intraepithelial and stromal telocytes established contact with macrophages either via
280 telopodes or the cell body (Fig. 4H, Fig.5 A, F, Fig. 11C, D). In control samples, few
281 macrophages were detected in the gill arches stroma (Fig. 7 A, B). Macrophages became
282 more active and were rich in lysosomes and vesicles in 6 ppt treated samples (Fig. 4 F-
283 H). In 10 ppt salinity level, large number of macrophages in gill arches stroma (Fig. 5 A-
284 F) and epithelial lymphatic spaces (Fig. 5C, Fig. 7E, F). In 14 ppt treated samples,
285 massive lysosomal-rich macrophages were observed in the stroma and epithelial
286 lymphatic spaces (Fig 6B, Fig. 7G).

287

288 Telopodes of several telocytes wrapped around stem cells and partially enclosed the stem
289 cell. Telopodes formed a planar contact along the cell membrane of the stem cell,
290 telopodes gave rise small branches extended into the cytoplasm of stem cell (Fig. 11 A,

291 B). Telocytes and their telopodes surrounded and established direct contact with the
292 skeletal myoblast (Fig. 11 C, E, F). Telopodes also formed contact with Schwann cells
293 (Fig. 11 C, D).

294

295 Intraepithelial and stromal telocytes formed contact with immature rodlet cells (granular
296 rodlet cells) (Fig. 4 F-H, Fig. 5A-D, Fig. 9A, B). Telocytes shed secretory vesicles and
297 multi-vesicular body in the vicinity of immature rodlet cells (Fig. 9A, B). The secretory
298 vesicles of the telocytes were observed in the surface epithelium (Fig. 9 C, D).
299 Intraepithelial telocytes established planar contact with pavement cell (Fig. 9E). In
300 control samples, Pavement cells were flattened with short microvilli (Fig 4A). Pavement
301 cells undergo modifications in salinity treated samples They enlarged in 6 ppt treated
302 samples (Fig. 9C). In 10 ppt salinity concentration, they were cuboidal in shape (Fig.
303 9E). Pavement cells became elongated and appeared columnar-shaped in 14 ppt level of
304 salinity (Fig. 6A). The micro-ridges became thin, elongated and extended beyond the
305 epithelial surface. Micro-ridges could be seen attached to or enclosing the secretory
306 vesicles of the telocytes. The surface of pavement cells formed pit-like invaginations
307 (Fig. 6 C, D).

308

309 Intraepithelial telocytes established planer contact with Chloride cells (Fig. 5D, 6C).
310 Chloride cells undergo structural modifications during elevation the level of the senility.
311 By TEM, they enlarged, and increase in number gradually depending on salinity
312 concentration. the mitochondrial number increased and changed their morphology from
313 rounded or oval in control group to elongated cigar-shaped in treated samples. Chloride

314 delivered the secretory vesicles of telocytes which were transferred through the intra-
315 epithelial lymphatic space (Fig 10 A-D, Fig. 5C, Fig. 6A). Amount of mitochondria in the
316 chloride cells was also evaluated by using Heidenhain's Iron-Hx. Mitochondria appeared
317 as black granules which increased with the level of the salinity (Fig. 3E-H).

318

319

320

321 **Discussion**

322 The current investigation was carried out to evaluate telocyte response to salinity stress
323 and their relation to osmoregulatory and immune cells. We detected telocytes in semi-
324 thin sections using toluidine blue, methylene blue and Heidenhain's Iron-Hx, and ultra-
325 thin sections to examine ultrastructural modifications in telocytes in relation to epithelial
326 and stromal cells.

327

328 In the current study, telocytes undergo morphological alternations during salinity stress.
329 They were spindle-shaped with fine telopodes in control samples. No significant changes
330 occurred in telocytes in 6 ppt salinity levels, while some telocytes exhibited higher
331 secretory activities. Telocytes shed large secretory vesicles, some populations of
332 telocytes had enlarged cell body, and telopodes became thicker and formed an extensive
333 network, in samples treated with 10 and 14 ppt salinity levels. Hormonal administration
334 could affect the secretory activities of telocytes. Exaggerated secretory activities of
335 telocytes are documented in melatonin treatment of ram seminal vesicles (**Abd-Elhafeez,**
336 **Mokhtar et al. 2016**).

337

338 In the current study, two types of telocytes were detected in the gills of common carp
339 according to location; intraepithelial telocytes and stromal telocytes. Telopodes formed
340 homocellular and heterocellular contacts. Heterocellular contact was established with a
341 wide range of cells and structures.

342

343 Intraepithelial telocytes communicated to from labyrinth network which comprised the
344 wall of the lymph spaces. These spaces represented interconnected channels interspersed
345 between epithelial cells. Intraepithelial telocytes shed their secretory vesicles and multi-
346 vesicular bodies in the intraepithelial lymph space which deliver them to other epithelial
347 and immune cells including chloride, pavement, mucous, rodlet cells and macrophages.
348 Intraepithelial telocytes may also establish contact with epithelial and immune cells either
349 via point or planar contact. Intraepithelial telocyte is previously detected by scanning
350 electron microscopy in the bovine uterine tube. telocyte is located in the basal layer of the
351 epithelial cells and their telopodes extended between epithelial cells (**Abd-Elhafeez and**
352 **Soliman 2016**)

353

354 In the current study, intercellular communication between telocytes chloride cells either
355 by direct contact or paracrine mode revealed that telocyte may have a potential role in
356 osmoregulation. Changing salinity level affect telocytes morphology which in turn
357 influence chloride cells. They undergo hypertrophy, change morphology of mitochondria
358 and increase their number upon elevation of the salinity level. similar results are
359 documented in the Hawaiian goby (*Stenogobius hawaiiensis*). Salinity caused a slight
360 increase in chloride cell number and size (**McCormick, Sundell et al. 2003**). Gill

361 chloride cells regulate ionic transportation via transport proteins which have a polarized
362 distribution. Three types of transport protein are described in chloride cells; cystic
363 fibrosis transmembrane regulator (CFTR) anion channel, Na,K,2Cl cotransporter
364 (NKCC) and sodium pump (Na,K-ATPase). Expression of Na⁺/K⁺-ATPase,
365 Na⁺/K⁺/2Cl⁻ cotransporter (NKCC) and cystic fibrosis transmembrane conductance
366 regulator (CFTR) in gill chloride cells of the Hawaiian goby (*Stenogobius hawaiiensis*) is
367 variant in freshwater and 20 per thousand and 30 per thousand salinity concentration for
368 10 days. Na⁺/K⁺-ATPase and NKCC have a basolateral/tubular localization whereas,
369 CFTR expressed in the apical surface of chloride cells. Gill Na⁺/K⁺-ATPase expression
370 is not affected by salinity, while CFTR immunoreactivity increase in salinity
371 **(McCormick, Sundell et al. 2003).**

372

373 In the present study, pavement cells were connected with telocytes. The secretory
374 vesicles could reach the surface epithelium and attached or partially enclosed by the
375 micro-ridges of the pavement cells. These cells were flattened in the control samples and
376 gradually enlarged depending on salinity level till became columnar-shaped in 14 ppt
377 salinity concentration. Micro-ridges became thinner and elongated in 10 and 14 salinity
378 levels. Pavement cells developed surface invaginations at 14 ppt salinity. A similar result
379 is described in the gill epithelia of the Adriatic sturgeon *Acipenser naccarii*. Pavement
380 cells acquired a complex system of microridges on their apical surface during exposure to
381 the hypertonic environment (salinity 35) **(CARMONA, GARCIA- GALLEGO et al.**
382 **2004)**. Pavement cells play an important role in gas exchange **(Evans, Claiborne et al.**

383 **2013**). They were rich in proton pumps which regulate acid-based balance (**Laurent,**
384 **Goss et al. 1994; Perry and Fryer 1997**).

385

386 In the current study, common carp couldn't sustain salinity levels more than 10 ppt. High
387 mortality rate in fish aquarium began in 12 ppt and was markedly increased in 14 ppt.
388 Mangat and Hundal investigated salinity effect on *Cyprinus carp* survival in different
389 seasons. They used 0, 1.5, 3, 6, and 12 ppt for 60 days. All fish are viable and survive at 0
390 ppt to 6 ppt salinity during all seasons. Only 50% survive at 12 ppt salinity during winter
391 (14.50C-19.00C), while Fish mortality percentage reached 100% during summer
392 (28.00C-37.00C) and autumn (22.50C-30.50C) (**Mangat and Hundal 2014**).

393

394

395 In the current study, both intraepithelial and stromal telocytes maintained relation with
396 immune cells; particularly macrophages and rodlet cells; either by cellular contact and
397 paracrine signaling. Thus, telocytes could maintain and enhance immune response in
398 different salinity levels. Macrophages increased in size, number and acquired exaggerated
399 phagocytic activities in samples treated with 14 ppt salinity level. They enlarged and
400 became rich in lysosomes and vesicles. Connection of telocytes and macrophage is
401 documented in mouse eye and rat urinary tract (**Zheng, Zhu et al. 2012; Luesma,**
402 **Gherghiceanu et al. 2013**). The contact point is identified by an electron-dense
403 nanostructure in the human heart (**Gherghiceanu and Popescu 2012**). Mouse peritoneal
404 macrophages are activated and secrete macrophage cytokines and enzymes when co-
405 cultured in telocytes conditioned media (**Chi, Jiang et al. 2015**). Macrophage activity is
406 investigated in relation to salinity level and ration. Phagocytic activities of the

407 macrophages of black sea bream; *Mylio macrocephalus* Basilewsky juveniles are
408 primarily affected by ration size rather than salinity (**Narnaware, Kelly et al. 2001**).

409

410 In the current study, telocytes formed a planar contact with the stem cell, some telopodes
411 extended into the cytoplasm of stem cell. Moreover, telocytes and their telopodes
412 enclosed and established direct contact with the skeletal progenitor cell which began
413 organization of the intracellular myofilament proteins. Relations between telocytes and
414 stem cells is mentioned in the heart (**Popescu, Curici et al. 2015**), lung, skeletal muscle,
415 meninges, and choroid plexus (**Popescu and Nicolescu 2013**). Cardiac telocytes
416 secrete cytokines and growth factors which promote stem cell proliferation and
417 differentiation such as interleukin (IL)-6, IL-2, IL-10, IL-13, VEGF, macrophage
418 inflammatory protein 1 α (MIP-1 α), MIP-2 and MCP-1 and some chemokines like, GRO-
419 KC (**Albulescu, Tanase et al. 2015**).

420

421 The present study provided evidence for relations of intraepithelial and stromal telocytes
422 with immature rodlet cells (granular stage). Telocytes exert their effect on rodlet cells
423 either through direct contact or paracrine signaling. Telocytes modified responding to
424 high salinity and subsequently affect rodlet cells. They were increased in number in
425 samples exposed 6, 10 and 14 ppt salinity. Thus, we suggested that telocytes may have a
426 role regulation of the biological activities and in maturation of rodlet cells. Many
427 researches are conducted to investigate the nature and function of rodlet cells. Rodlet
428 cells are thought to act as ion transporting cells and involve in osmoregulation
429 (**Ostrander 2000**). The widely acceptable hypothesis is that rodlet cells participate in

430 immune response. They are common in helminthic infestations and other noxious agents
431 and considered as a type of eosinophilic granulocyte (**Reite and Evensen 2006; Matisz,**
432 **Goater et al. 2010**). Rodlet cells undergo significant changes depending on salinity
433 level. They are increased during reduction of salinity in European sea bass *Dicentrarchus*
434 *labrax* (**Giari, Manera et al. 2006**).

435

436 In the present study, stromal telocytes established a direct contact with secondary
437 vascular vessels or lymph vessels. The secretory vesicles of the stromal telocytes were
438 secreted in lymph vessel. Lymphatic vessels deliver the inflow from arterial vessels via
439 arterio-arterial anastomoses and drain into the venous circulation (**Kapoor and Bhavna**
440 **2004**). Thus, we suggested that the secondary vascular vessels represented a principal
441 pathway for trafficking of telocytes sections in the blood circulation. Thus, telocytes may
442 exert their paracrine effect on remote tissues and organs. The secondary vascular vessels
443 are implicated in gaseous exchange and ion transportation (**Steffensen and Lomholt**
444 **1992**).

445

446 In conclusion, fish body accommodated changing level of the salinity by activation of an
447 adaptive response through cellular communications. Telocytes represented a major
448 component in the communicating system. They regulated the function of a wide variety
449 of cells either by direct contact or paracrine mode. Morphological modification of
450 telocytes in different levels of salinity reflected increase their activities which influence
451 epithelial, immune and stromal effector cells. Intraepithelial telocytes affected chloride,
452 pavement cells, immature rodlet cells and macrophages while stromal telocytes influence

453 stem cells, skeletal myoblasts and also macrophages and rodlet cells. Thus, telocytes
454 enhanced immunity, osmoregulation in gill lamellar and filament epithelium and
455 regeneration of stromal cells. Thus, the fish could sustain hyperosmotic environments
456 reaching 10 ppt and maintain internal homeostasis.

457

458 **References**

- 459 Abd-Elhafeez, H. H., Mokhtar, D. M., Hassan, A. H. (2016). Effect of Melatonin on
460 Telocytes in the Seminal Vesicle of the Soay Ram: An Immunohistochemical,
461 Ultrastructural and Morphometrical Study. *Cells Tissues Organs*.
462 Abd-Elhafeez, H. H., Soliman, S. A. (2016). New Description of Telocyte Sheaths in the
463 Bovine Uterine Tube: An Immunohistochemical and Scanning Microscopic Study. *Cells*
464 *Tissues Organs*.
465 Albuлесcu, R., Tanase, C., Codrici, E., Popescu, D. I., Cretoiu, S. M., Popescu, L. M.
466 (2015). The secretome of myocardial telocytes modulates the activity of cardiac stem
467 cells. *J Cell Mol Med* 19(8):1783-1794.
468 Bancroft, J. D., Layton, C., Suvarna, S. K. (2013). *Bancroft's Theory and Practice of*
469 *Histological Techniques*. . Churchill Livingstone; 7 edition.
470 Bei, Y., Wang, F., Yang, C., Xiao, J. (2015). Telocytes in regenerative medicine. *J Cell*
471 *Mol Med* 19(7):1441-1454.
472 Cantarero Carmona, I., Luesma Bartolome, M. J., Junquera Escribano, C. (2011).
473 Identification of telocytes in the lamina propria of rat duodenum: transmission electron
474 microscopy. *J Cell Mol Med* 15(1):26-30.
475 CARMONA, R., GARCIA- GALLEGO, M., SANZ, A., DOMEZAIN, A., OSTOS-
476 GARRIDO, M. V. (2004). Chloride cells and pavement cells in gill epithelia of
477 *Acipenser naccarii*: ultrastructural modifications in
478 seawater-acclimated specimens. *Journal of Fish Biology* 64:553–566.
479 Chi, C., Jiang, X. J., Su, L., Shen, Z. J., Yang, X. J. (2015). In vitro morphology,
480 viability and cytokine secretion of uterine telocyte-activated mouse peritoneal
481 macrophages. *J Cell Mol Med* 19(12):2741-2750.
482 Derichs, N. (2013). Targeting a genetic defect: cystic fibrosis transmembrane
483 conductance regulator modulators in cystic fibrosis. *Eur Respir Rev* 22(127):58-65.
484 Drumm, B. T., Koh, S. D., Andersson, K. E., Ward, S. M. (2014). Calcium signalling in
485 Cajal-like interstitial cells of the lower urinary tract. *Nat Rev Urol* 11(10):555-564.
486 Evans, D. H., Claiborne, J. B., Currie, S. (2013). *The Physiology of Fishes*, Fourth
487 Edition. CRC Press:152.
488 Fielder, D. S., Allan, G. L., Pepperall, D., Pankhurst, P. M. (2007). The effects of
489 changes in salinity on osmoregulation and chloride cell morphology of juvenile
490 Australian snapper, *Pagrus auratus*. . *Aquaculture* 272:656-666.
491 Florkin, M. (2014). *Deuterostomians, Cyclostomes, and Fishes*. Elsevier:166.

- 492 Gandahi, J. A., Chen, S. F., Yang, P., Bian, X. G., Chen, Q. S. (2012). Ultrastructural
493 identification of interstitial cells of Cajal in hen oviduct. *Poult Sci* 91(6):1410-1417.
- 494 Gherghiceanu, M., Hinescu, M. E., Andrei, F., Mandache, E., Macarie, C. E., Faussone-
495 Pellegrini, M. S., Popescu, L. M. (2008). Interstitial Cajal-like cells (ICLC) in
496 myocardial sleeves of human pulmonary veins. *J Cell Mol Med* 12(5A):1777-1781.
- 497 Gherghiceanu, M., Popescu, L. M. (2012). Cardiac telocytes - their junctions and
498 functional implications. *Cell Tissue Res* 348(2):265-279.
- 499 Giari, L., Manera, M., Simoni, E., Dezfuli, B. S. (2006). Changes to chloride and rodlet
500 cells in gills, kidney and intestine of *Dicentrarchus labrax* (L.) exposed to reduced
501 salinities. *Journal of Fish Biology* 69(2):590-600.
- 502 Heidenhai, N. M. (1896). Noch einmal uber die Darstellung der centralkorper durch
503 Eisenhamatoxylin nebst einigen allgemeinen Bemerkungen uber die Hamatoxylin
504 fabren. *Zeitschrift fur wissenschaftliche Mikroskopie und fur Mikroskopische Technik*
505 13:180.
- 506 Hutchings, G., Williams, O., Cretoiu, D., Ciontea, S. M. (2009). Myometrial interstitial
507 cells and the coordination of myometrial contractility. *J Cell Mol Med* 13(10):4268-
508 4282.
- 509 Iino, S., Horiguchi, K. (2006). Interstitial cells of Cajal are involved in neurotransmission
510 in the gastrointestinal tract. *Acta Histochem Cytochem* 39(6):145-153.
- 511 Kapoor, B. G., Bhavna, K. (2004). *Ichthyology Handbook*. Springer Science & Business
512 Media:289.
- 513 Laurent, P., Goss, G. G., Perry, S. F. (1994). Proton pumps in fish gill pavement cells?
514 *Arch Int Physiol Biochim Biophys* 102(1):77-79.
- 515 Lloyd, R. V. (2001). *Morphology Methods: Cell and Molecular Biology Techniques*.
516 Springer Science & Business Media.
- 517 Luesma, M. J., Gherghiceanu, M., Popescu, L. M. (2013). Telocytes and stem cells in
518 limbus and uvea of mouse eye. *J Cell Mol Med* 17(8):1016-1024.
- 519 Mangat, H. K., Hundal, S. S. (2014). Salinity tolerance of laboratory reared fingerlings
520 of common carp, *Cyprinus carpio* (Linn.) during different seasons. *International Journal*
521 *of Advanced Research* 2(11):491-496.
- 522 Marshall, W. S., Grosell, M. (2005). Ion transport, osmoregulation and
523 acid-base balance.
524 . In *Physiology of Fishes 3*, (ed. D. Evans and J. B. Claiborne):pp. 177-230. Boca Raton:
525 CRC Press.
- 526 Matisz, C. E., Goater, C. P., Bray, D. (2010). Density and maturation of rodlet cells in
527 brain tissue of fathead minnows (*Pimephales promelas*) exposed to trematode cercariae.
528 *Int J Parasitol* 40(3):307-312.
- 529 McCormick, S. D., Sundell, K., Bjornsson, B. T., Brown, C. L., Hiroi, J. (2003).
530 Influence of salinity on the localization of Na⁺/K⁺-ATPase, Na⁺/K⁺/2Cl⁻ cotransporter
531 (NKCC) and CFTR anion channel in chloride cells of the Hawaiian goby (*Stenogobius*
532 *hawaiiensis*). *J Exp Biol* 206(Pt 24):4575-4583.
- 533 Mirancea, N. (2016). Telocyte - a particular cell phenotype. Infrastructure, relationships
534 and putative functions. *Rom J Morphol Embryol* 57(1):7-21.
- 535 Narnaware, Y. K., Kelly, S. P., Woo, N. Y. S. (2001). Effect of salinity and ration size
536 on macrophage phagocytosis in juvenile black sea bream (*Mylio macrocephalus*).
537 *Journal of Applied Ichthyology* 16(2):86 - 88

- 538 Nelson, J. S. (2006). *Fishes of the World*. John Wiley & Sons, Inc 4th ed:140.
- 539 Ostrand, G. K. (2000). *The Laboratory Fish*. Elsevier:288.
- 540 Perry, S. F., Fryer, J. N. (1997). Proton pumps in the fish gill and kidney. *Fish*
541 *Physiology and Biochemistry* 17(1-6):363-369.
- 542 Popescu, L. M., Curici, A., Wang, E., Zhang, H., Hu, S., Gherghiceanu, M. (2015).
543 Telocytes and putative stem cells in ageing human heart. *J Cell Mol Med* 19(1):31-45.
- 544 Popescu, L. M., Fausone-Pellegrini, M. S. (2010). TELOCYTES - a case of serendipity:
545 the winding way from Interstitial Cells of Cajal (ICC), via Interstitial Cajal-Like Cells
546 (ICLC) to TELOCYTES. *J Cell Mol Med* 14(4):729-740.
- 547 Popescu, L. M., Gherghiceanu, M., Cretoiu, D., Radu, E. (2005). The connective
548 connection: interstitial cells of Cajal (ICC) and ICC-like cells establish synapses with
549 immunoreactive cells. Electron microscope study in situ. *J Cell Mol Med* 9(3):714-730.
- 550 Popescu, L. M., Nicolescu, M. I. (2013). Resident stem cells and regenerative therapy,
551 Chapter: Telocytes and stem cells, . Publisher: Oxford: Academic Press, Editors: dos
552 Santos Goldenberg RC, Campos de 7 Carvalho AC:205-231.
- 553 Reite, O. B., Evensen, O. (2006). Inflammatory cells of teleostean fish: a review
554 focusing on mast cells/eosinophilic granule cells and rodlet cells. *Fish Shellfish Immunol*
555 20(2):192-208.
- 556 Russell, J. M. (2000). Sodium-potassium-chloride cotransport. *Physiol Rev* 80(1):211-
557 276.
- 558 Steffensen, J. F., Lomholt, J. P. (1992). *Fish Physiology XIIA - Circulation*, Chapter:
559 The secondary vascular system. . Publisher: Academic Press, Editors: Hoar, W. S.
560 Randall, D. J. & Farrell, A. P:185-217.
- 561 Suhail, M. (2010). Na, K-ATPase: Ubiquitous Multifunctional Transmembrane Protein
562 and its Relevance to Various Pathophysiological Conditions. *J Clin Med Res* 2(1):1-17.
- 563 Takaki, M. (2003). Gut pacemaker cells: the interstitial cells of Cajal (ICC). *J Smooth*
564 *Muscle Res* 39(5):137-161.
- 565 Varga, I., Danisovic, L., Kyselovic, J., Gazova, A., Musil, P., Miko, M., Polak, S. (2016).
566 The functional morphology and role of cardiac telocytes in myocardium regeneration.
567 *Can J Physiol Pharmacol*:1-5.
- 568 Zheng, Y., Zhu, T., Lin, M., Wu, D., Wang, X. (2012). Telocytes in the urinary system.
569 *J Transl Med* 10:188.

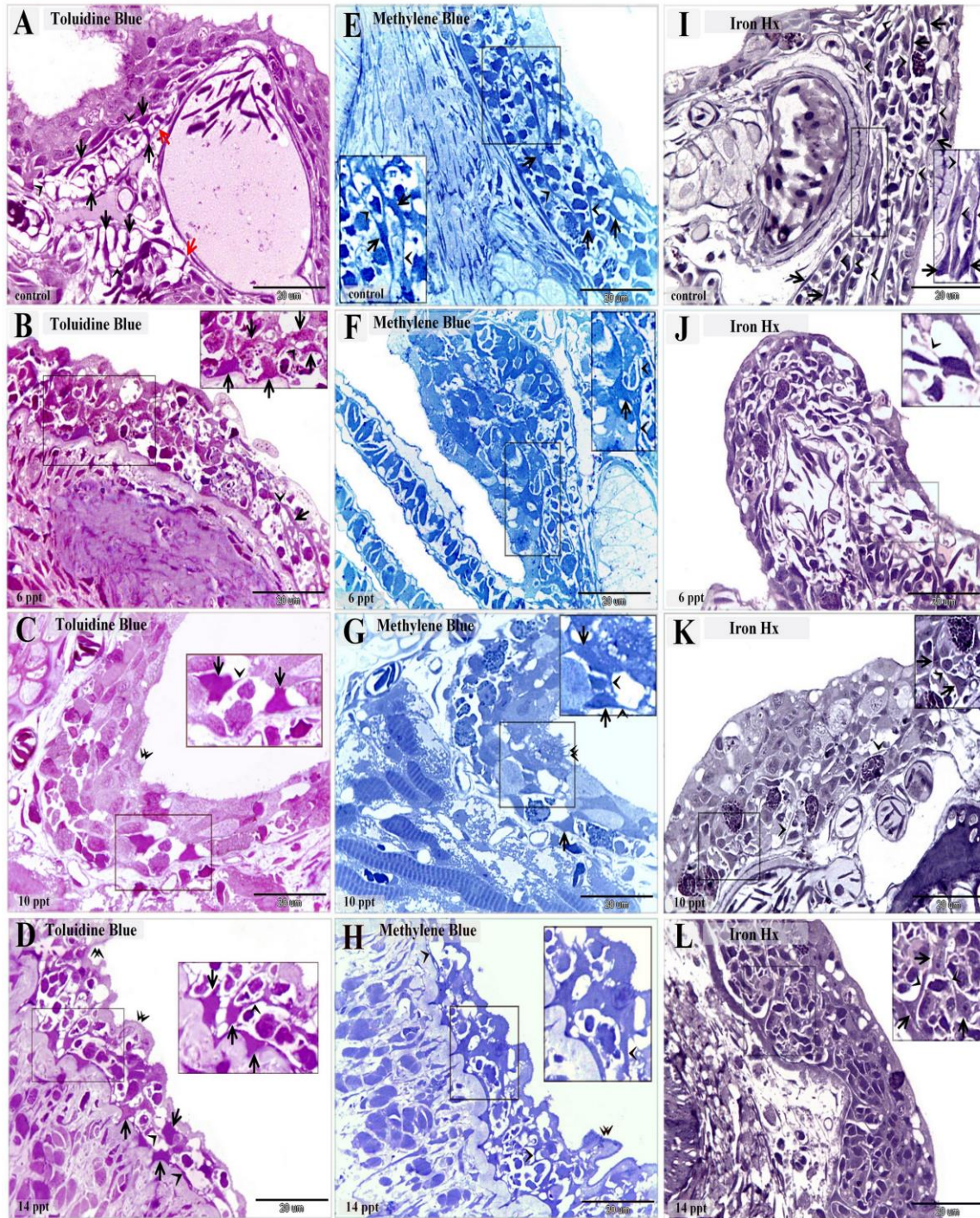
570

571

572

573

574

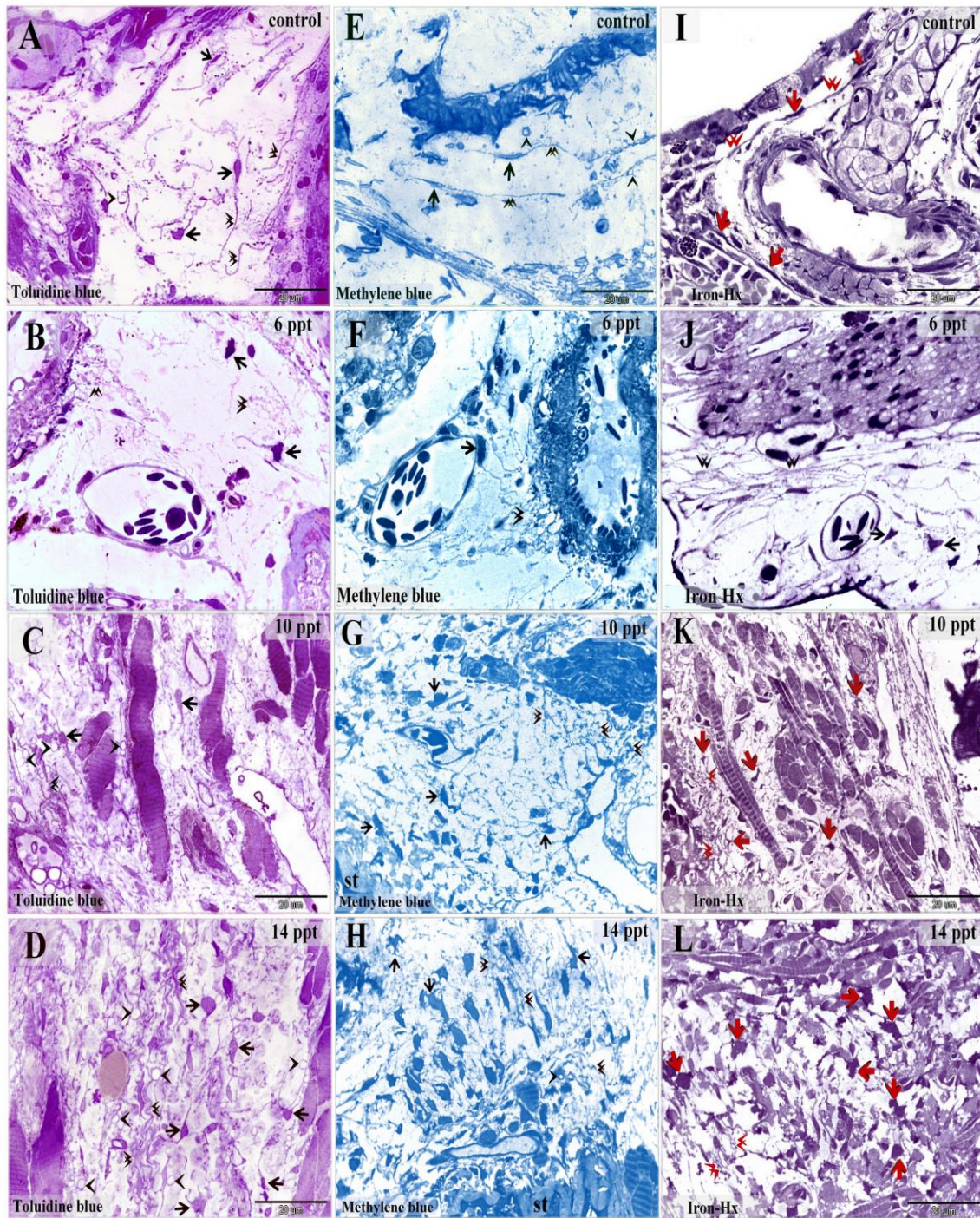


575

576 **Figure 1: Morphological changes of the intraepithelial telocytes responding to**
577 **salinity**

578 Semi-thin sections of gill arches and filaments stained with toluidine blue (A-D),
579 methylene blue (E-H) and Heidenhain's Iron-Hx (I-L). A, E, I: showed intraepithelial

580 telocytes in control samples. They had small cell body (arrows) and prominent telopodes
581 (arrowheads). Note the red arrows refer to the basal lamina. B, F, J: showed
582 intraepithelial telocytes during exposure to 6 ppt salinity level. The cell body enlarged
583 and were satellite in shape (arrows). Note telopodes (arrowheads). C, G, K: cell body
584 undergo hypertrophy and became large satellite (arrows) of the intraepithelial telocytes
585 exposed to 10 ppt salinity level. Note telopodes (arrowheads). D, H, L: the cell body
586 (arrows) of the intraepithelial telocytes increased in size in 14 ppt salinity level. Note
587 telopodes (arrowheads).
588

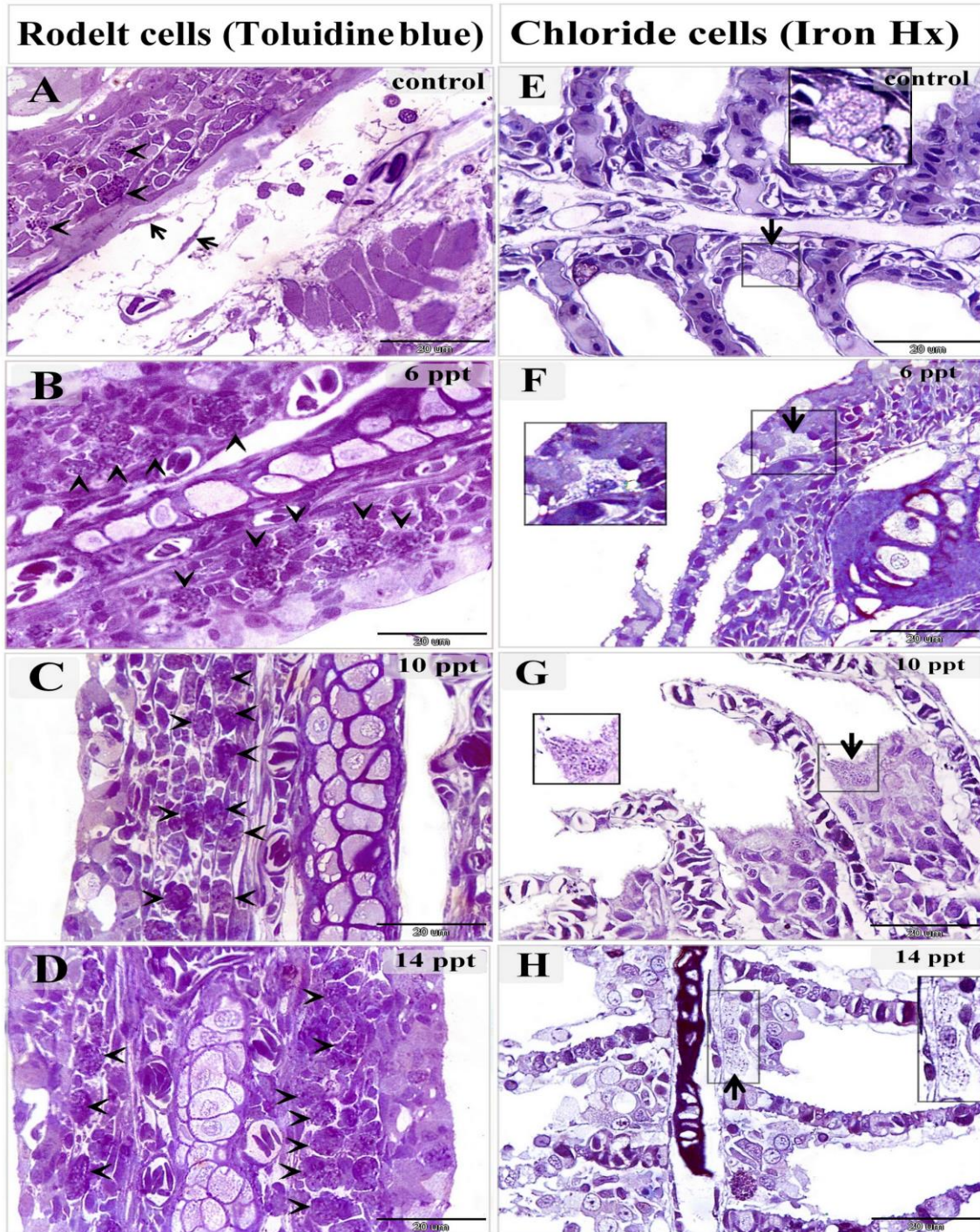


589

590 **Figure 2: Morphological changes of the stromal telocytes responding to salinity**

591 Semi-thin sections of gill arches and filaments stained with toluidine blue (A-D),
592 methylene blue (E-H) and Heidenhain's Iron-Hx (I-L). A, E, I: showed stromal telocytes
593 in control samples. They had small cell body (arrows) associated with long telopodes
594 (double arrowheads) . Note the secretory vesicles (arrowheads). B, F, J: Some stromal

595 telocytes had enlarged cell body (arrows) during exposure to 6 ppt salinity level. Note
596 telopodes formed a network (double arrowheads). C, G, K: stromal telocytes (arrows)
597 exposed to 10 ppt salinity level had an extensive network of telopodes (double
598 arrowheads) Note the secretory vesicles (arrowheads). D, H, L: stromal telocytes
599 (arrows), telopodes (double arrowheads). Note the secretory vesicles (arrowheads).
600



601

602 **Figure 3: Changes of rodlet and chloride cells responding to salinity stress**

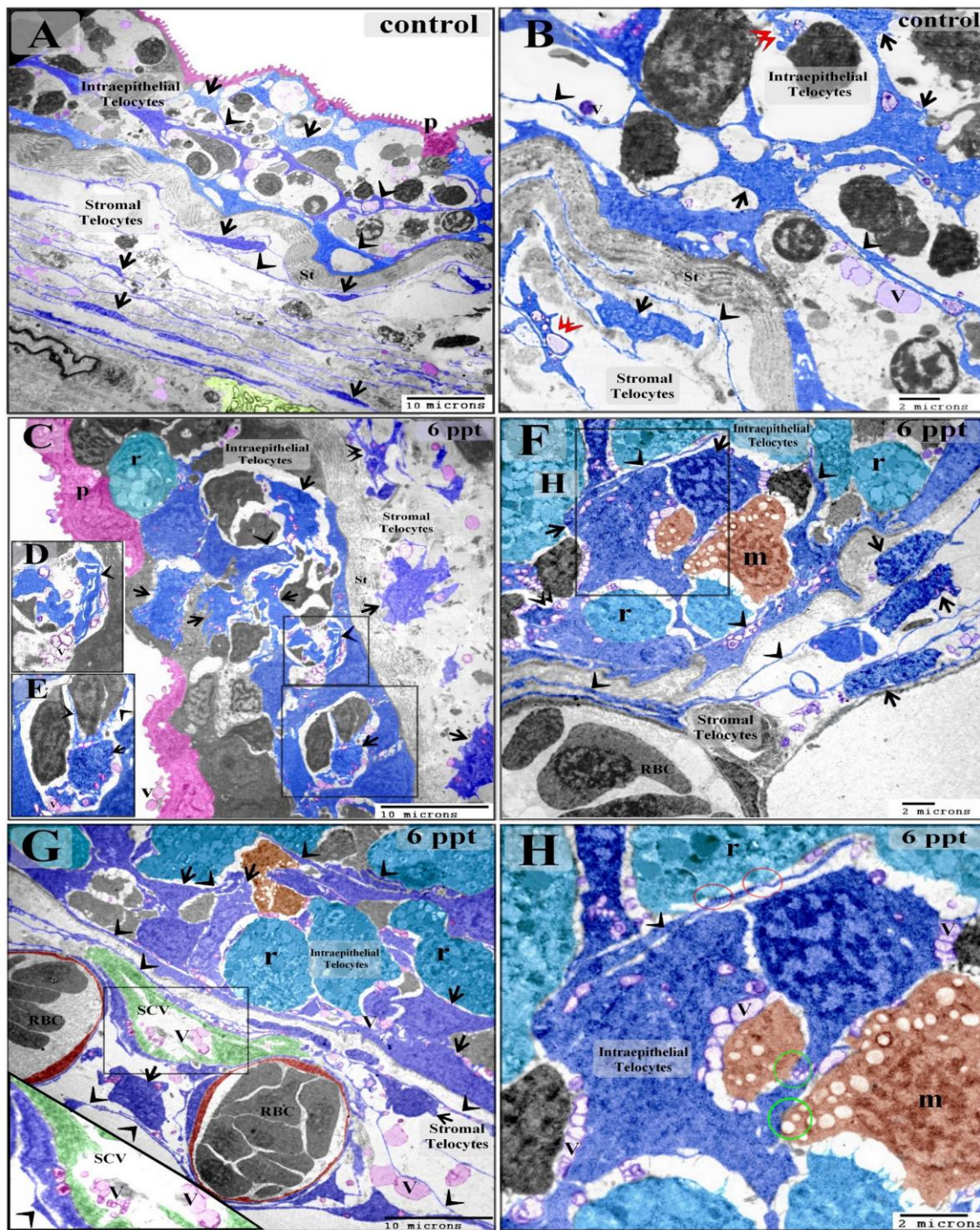
603 Semi-thin sections of gill arches and filaments stained with toluidine blue (A-D), and

604 Heidenhain's Iron-Hx (E-H). A: few number of immature rodlet cells (granular stage)

605 (arrowheads) in control samples. B: Number of immature rodlet cells (arrowheads)

606 increased in branchial epithelium in 6 ppt treated samples. C: Enormous number of rodlet

607 cells (arrowheads) in branchial epithelium exposed to 10 ppt salinity level. D: Massive
608 number of rodlet cells (arrowheads) in branchial epithelium in 14 ppt treated samples. E:
609 chloride cell (arrow) in control samples was small contained few mitochondria which
610 appeared as dark dots by iron Hx stain. F: large chloride cells (arrow) in 6 ppt treated
611 samples had larger number of mitochondria. G: Chloride cell (arrow) enlarged and
612 contained abundant mitochondria in 10 ppt treated samples. H: hypertrophy of the
613 chloride cells with massive mitochondrial content in 14 ppt salinity level.
614

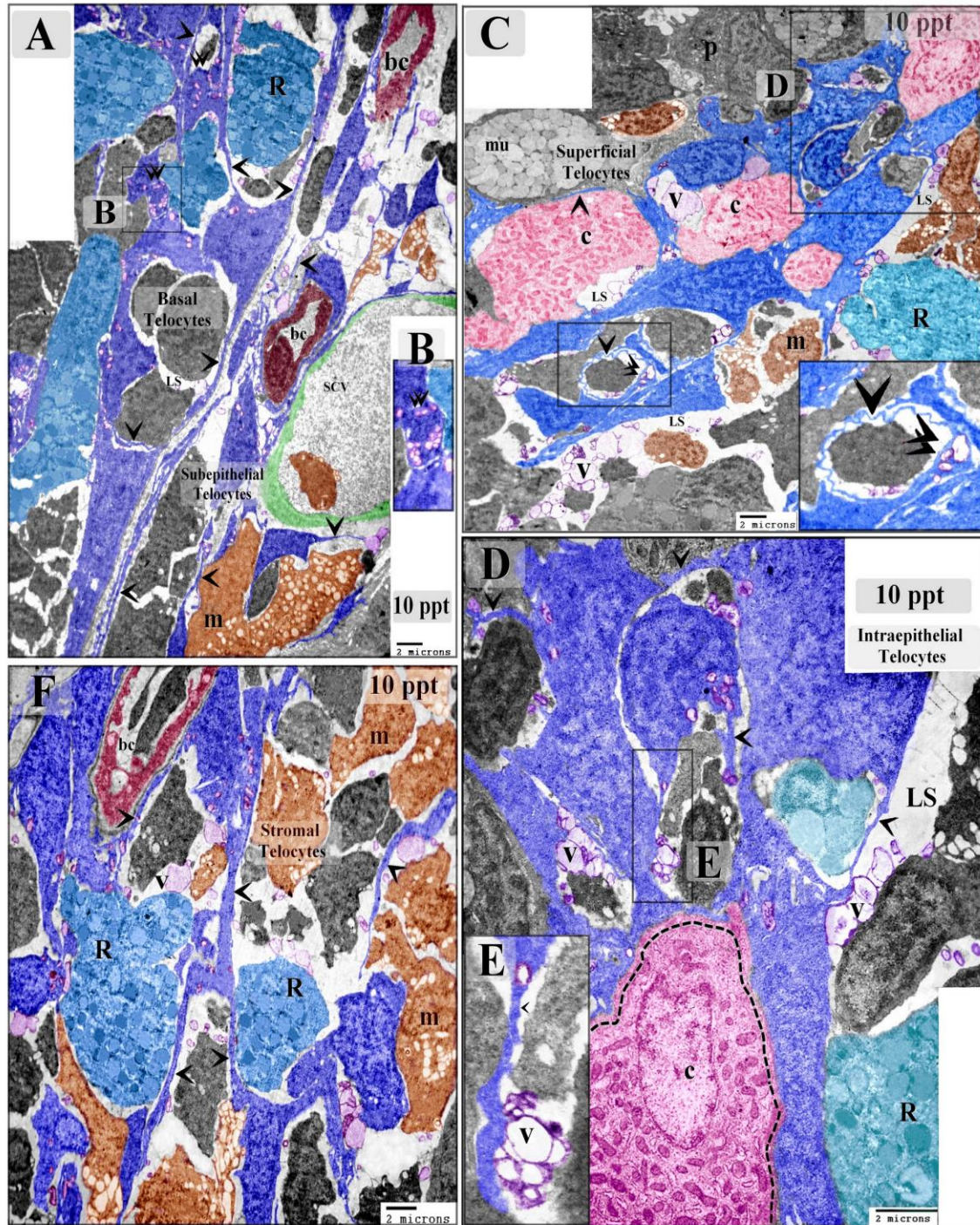


615

616 **Figure 4: effect of low level (6 ppt) of salinity on intraepithelial telocytes.**

617 Colored ultra-thin sections in gill arches (A-F, H) and filaments (G) of control (A, B) and
618 6 ppt treated samples (C-H). A, B: intraepithelial telocytes were small, had spindle or
619 satellite-shaped (arrows) and thin telopodes (arrowheads). They rest on the basal lamina
620 which directly opposed on the stratum compactum (st). They organized in a labyrinth

621 network which comprised the wall of the epithelial lymph spaces. The secretory vesicles
622 (V) were liberated in the lymph spaces. Note podoms (double arrowheads), pavement
623 cells (P). stromal telocytes had longer and thinner telopodes. C-H: Enlargement of the
624 both intraepithelial and stromal telocytes (arrows), thickening of the telopodes
625 (arrowheads). intraepithelial telocytes liberated the secretory vesicles in the lymph spaces
626 and stromal telocytes shed their vesicles in the secondary circulatory vessels (SCV) or
627 lymphatic vessels. Note stratum compactum (st), pavement cells (p). branchial blood
628 vessels contained red blood cells (RBC). Rodlet cells (r) and lysosome-rich macrophages
629 (m) in the lymph spaces. red circles refer to point of contact between telopodes and rodlet
630 cells, green circle refer to contact between telocytes and the macrophage in branchial
631 epithelium.
632

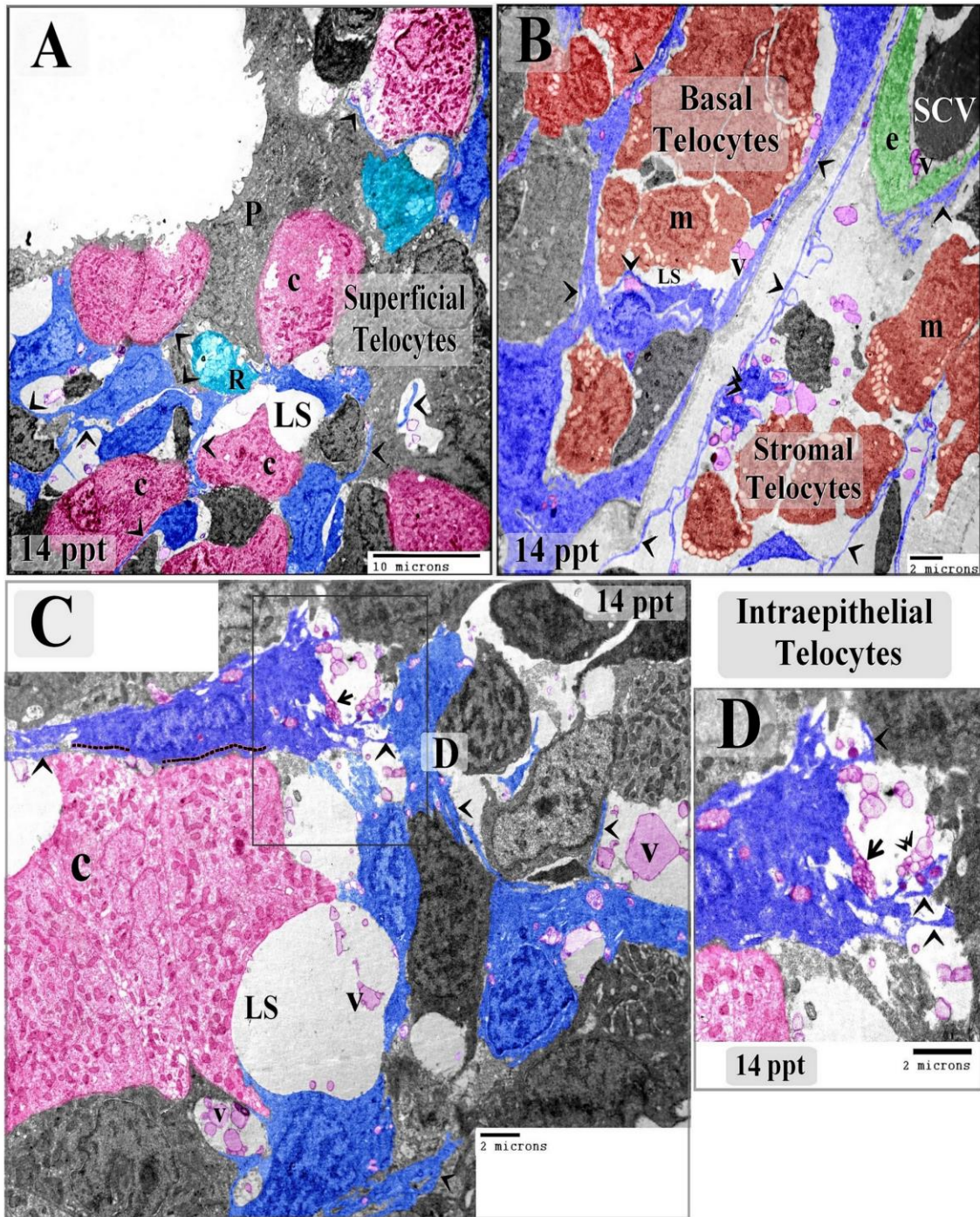


633

634 **Figure 5: effect of 10 ppt salinity level on intraepithelial telocytes.**

635 Colored ultra-thin sections in gill arches of 10 ppt treated samples. The prominent feature
636 in 10 ppt level treated samples was increase in size of telocytes either intraepithelial or
637 stromal. A: Basal telocytes were telocytes in the basal layer of the branchial epithelium
638 established a communicating network between the lymph spaces (LS) in which rodlet

639 cells (R) migrated. Note telopodes (arrowheads), podom (double arrowheads). The sub-
640 epithelial telocytes connected with blood capillaries (bc), secondary circulatory vessels
641 (SCV) and lysosome-rich macrophages (m). Both Basal intraepithelial and sub-epithelial
642 telocytes undergo hypertrophy. B: high magnification of the podom. C: Superficial
643 intraepithelial telocytes established contact with different types of epithelial cells and
644 formed the lymph spaces (LS) where they shed the secretory vesicles (V). Note telopodes
645 (arrowheads), podoms (double arrowheads). chloride cell (c), rodlet cells (R), pavement
646 cell (P), Mucous cell (mu), macrophages (m). D, E: intraepithelial telocytes established
647 planar contact with chloride cell (dashed line). Telocytes shed the numerous secretory
648 vesicles (V) in the lymph space (LS). Note telopodes (arrowheads). F: Stromal telocytes
649 formed a network connected with different types of stromal cells including rodlet cells
650 (R) and macrophages (m). note telopodes (arrowheads), blood capillary (bc).
651

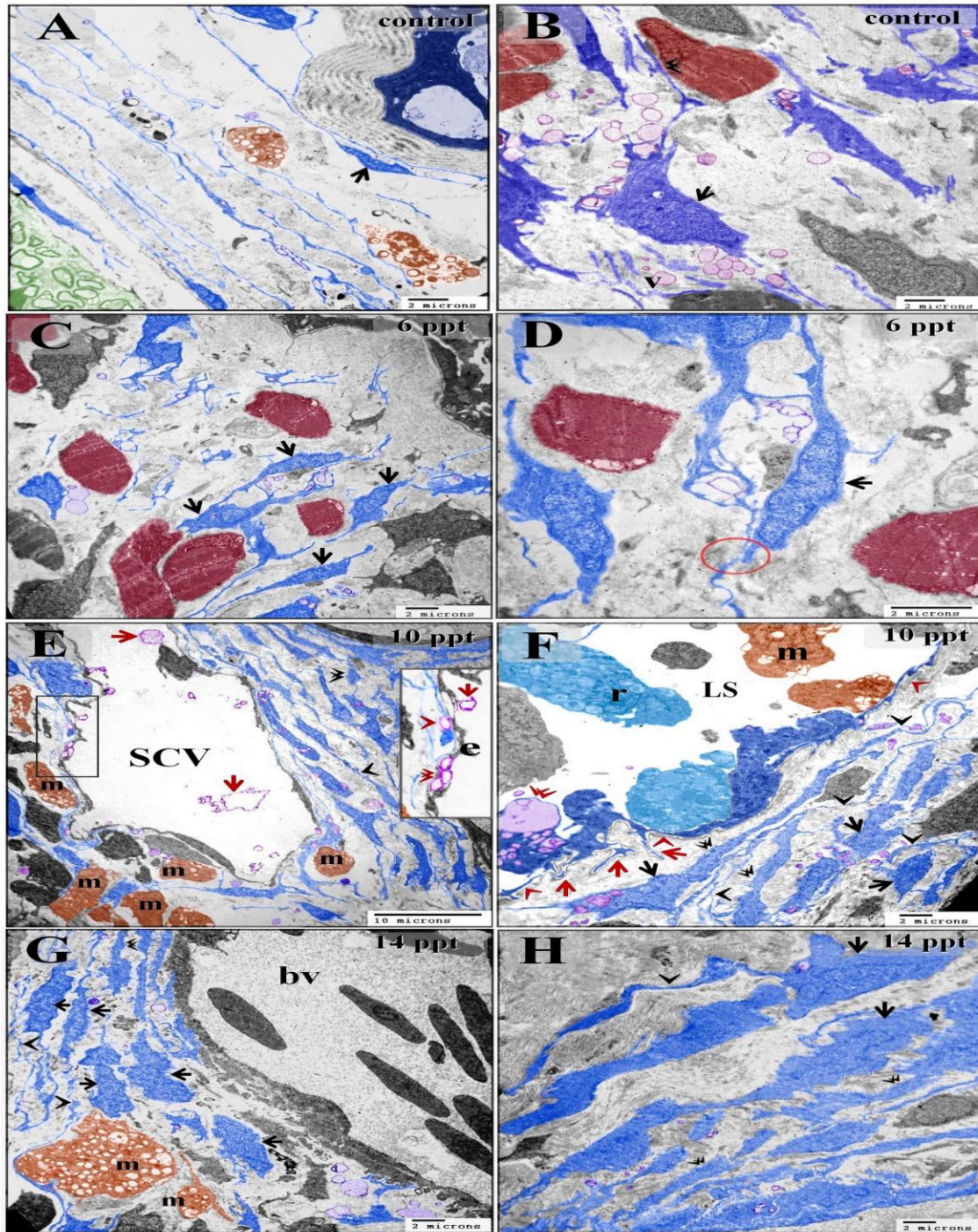


652

653 **Figure 6: effect of high salinity level (14 ppt) on intraepithelial telocytes**

654 Colored ultra-thin sections in gill arches of 14 ppt treated samples. A: Superficial
655 intraepithelial telocytes communicated forming a labyrinth network between epithelial
656 cells and established the lymph spaces (LS). Note telopodes (arrowheads), Chloride cells
657 (C), rodlet cells (R), pavement cell (P) with short microvilli. B: Basal telocytes organized

658 a network which enclose the lymph spaces (LS). massive number of macrophages (M) in
659 the lymph spaces. Telopodes (arrowheads). Stromal telocytes established contact with
660 secondary circulatory vessels (SCV), stromal macrophages (m). note podom (double
661 arrowhead). C, D: Intraepithelial telocytes formed a network between the epithelial cells
662 and construct the wall of the lymph spaces (LS). Note Intraepithelial telocytes formed a
663 planar contact (dashed line). The secretory vesicles and multivesicular body (arrow),
664 exosomes (double arrowhead) of the intraepithelial telocytes were shed in the lymph
665 spaces. Note telopodes (arrowheads).
666



667

668 **Figure 7: Effect of saintly on stromal telocytes**

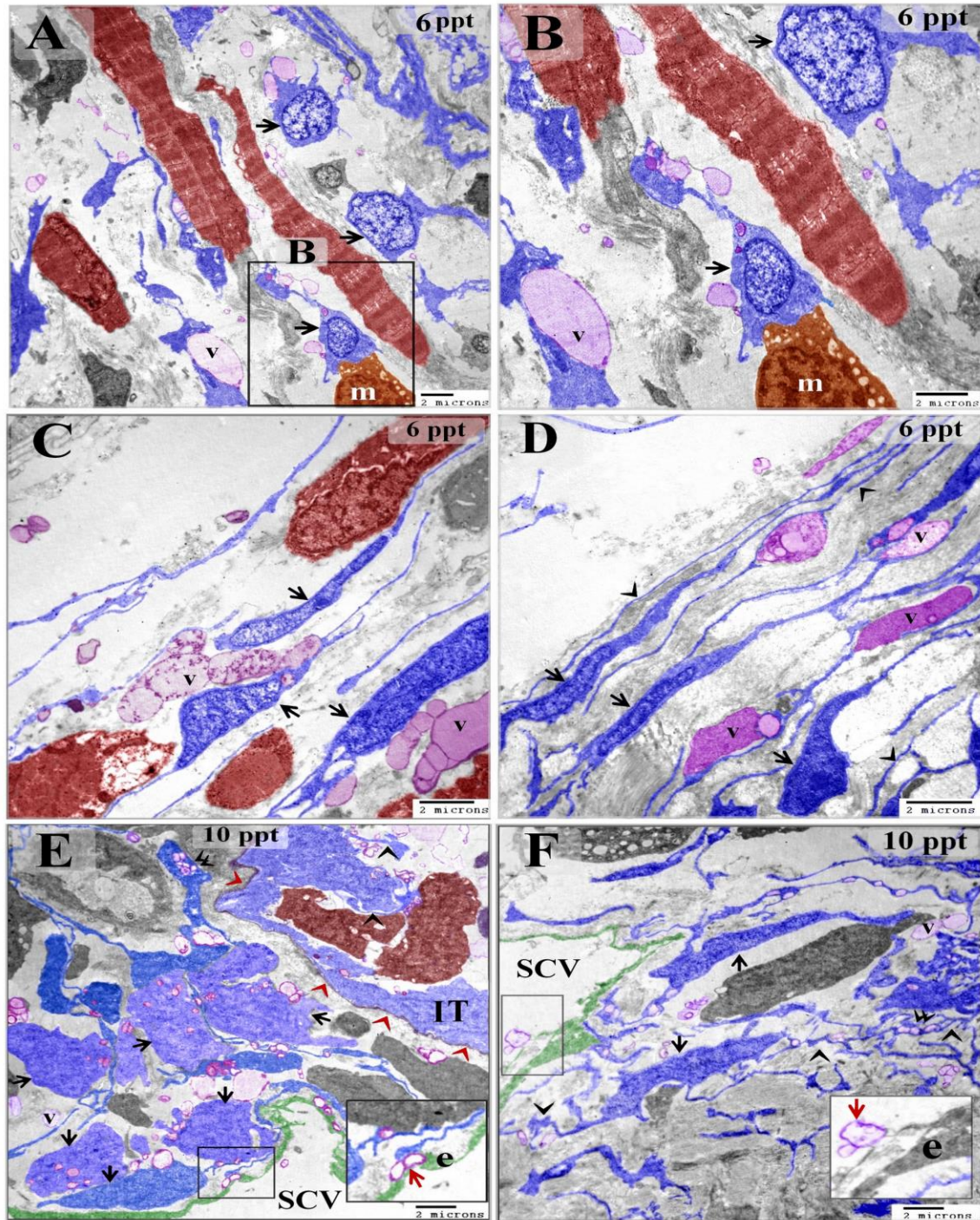
669 Colored ultra-thin sections in gill arches of control (A, B), 6 ppt (C, D), 10 ppt (E, F), 14

670 ppt (G, H) treated samples. A, B: telocytes appeared small spindle or satellite shaped

671 (arrows). Telocyte established direct contact with skeletal muscle (double arrowhead). C,

672 D: small spindle-shaped telocytes established homocellular junction (red circle). E: large

673 population of telocytes surrounding the secondary circulatory vessel (SCV). The
674 secretory vesicles (red arrowhead) of telocytes transferred through the endothelial lining
675 of the secondary circulatory vessel (red double arrowheads) and shed in the lumen of the
676 vessel (red arrows). note thick telopodes (black double arrowhead) and slight waving
677 (black arrowhead) of the telopodes shape, macrophages (m). F: subepithelial telocytes (
678 black arrows), telopodes became enormous (black arrowheads) telopodes undergo
679 thickening in certain areas (double arrowheads). The basal lamina (red arrowheads). Note
680 the basal intraepithelial telocytes gave rise short basal telopodes (red arrows). Note
681 podom of the basal intraepithelial telocyte (double arrowhead), lymph space (LS), rodlet
682 cells (r), macrophages (m). G, H: The most prominent features of high salinity changes
683 were the cell body had an irregular surface (arrows) and wavy telopodes (arrowheads)
684 and thickening of telopodes (double arrowhead) note macrophage (m) enlargement and
685 was filled with lysosomes (m), blood vessel (bv).
686

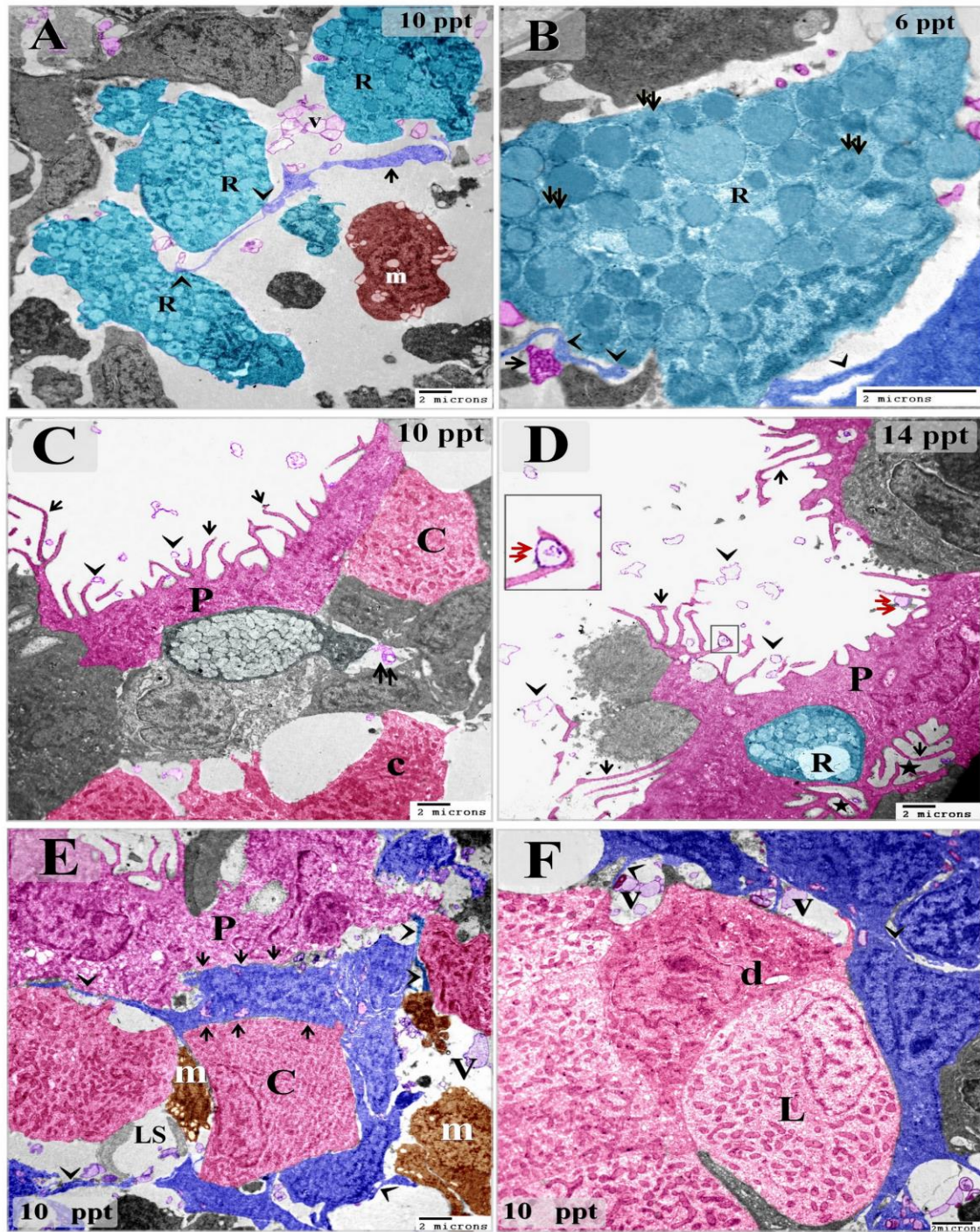


687

688 **Figure 8: Increase the secretory activities of the stromal telocytes responding to**
689 **salinity and liberation of the secretory vesicles in the secondary circulatory vessels.**

690 Colored ultra-thin sections in gill arches treated with 6 ppt (A-D) and 10 ppt (E, F) level
691 of salinity. A, B: enlarged telocytes acquired rounded or triangular shape (arrows). Note
692 large secretory vesicle (V), cell body of stromal telocyte established contact with

693 macrophage (m). C, D: spindle-shaped telocytes (arrows) shed large secretory vesicle
694 (V). note enormous telopodes (arrowheads). E: large number of enlarged subepithelial
695 telocytes (arrows). Podom (double arrow). Some telocytes established contact with the
696 endothelial lining of the secondary circulatory vessel (SCV). Note transferring of the
697 secretory vesicles (red arrow) secreted by telocytes to the cytoplasm of endothelial cells
698 (e). Basal lamina (red arrowheads). intraepithelial telocytes (IT) and their telopodes
699 (arrowheads). F: spindle shaped stromal telocytes (arrows) and their telopodes formed an
700 extensive network (arrows), podom (double arrowhead), the secretory vesicles (V). note
701 the secretory vesicles (red arrow) were observed in the lumen of the secondary
702 circulatory vessel (SCV). endothelial cells (e).
703



704

705 **Figure 9: Intraepithelial telocytes in relations to rodlet, chloride and pavement cells.**

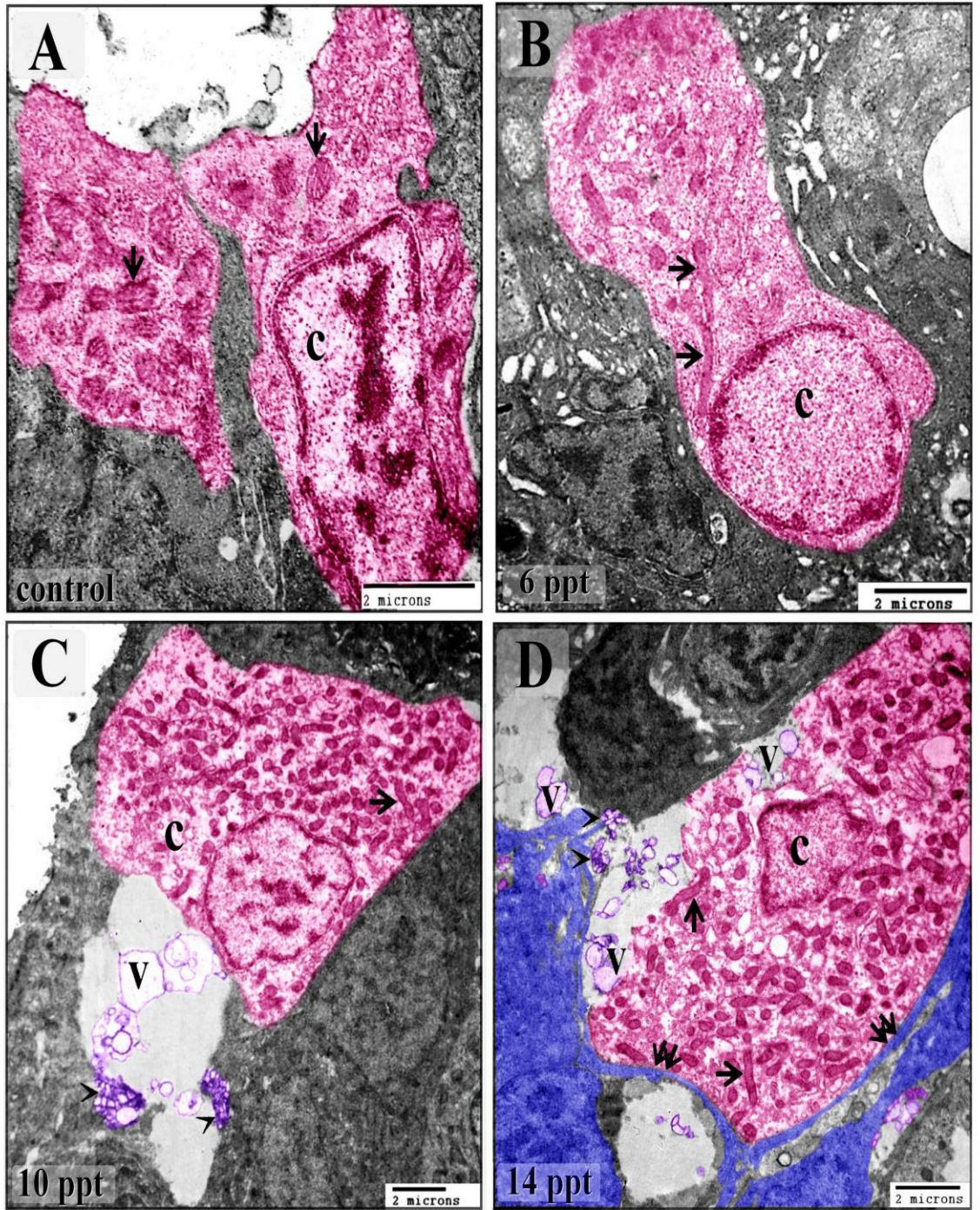
706 Colored ultra-thin sections in gill arches treated with 6 ppt (B),10 ppt (A, C, E, F) and 14

707 ppt (D) level of salinity. A: stromal telocytes (arrow) in direct contact with rodlet cells

708 (arrowheads). Note the telocytes shed the secretory vesicles (V) in vicinity to rodlet cells

709 (R). Macrophage (m). B: rodlet cell (granular stage) had immature rodlet granules

710 (double arrows) which contained an electron dense central core. Telopodes (arrowheads)
711 in contact with rodlet cell (R). note multi-vesicular body (arrow). C, D: some pavement
712 cells (P) in 10 and 14 ppt salinity samples had long microvilli (arrows) which deliver the
713 secretory vesicles (arrowheads) of telocytes at the surface of the branchial epithelium.
714 surface invaginations or pits (asterisk) in the pavement cells Note secretory vesicles in
715 lymph space (double arrow), chloride cells (C), rodlet cell (R). E: Intraepithelial telocyte
716 in planer contact (arrows) with the pavement cells (P) and chloride cell (C). note
717 Telopodes (arrows), macrophages (m), secretory vesicles (V), Lymph space (LS). F: two
718 types of mitochondrial rich chloride cells; dark (d) and light (L) were connected to
719 telocytes. Note telopodes (arrows), secretory vesicles (V).
720

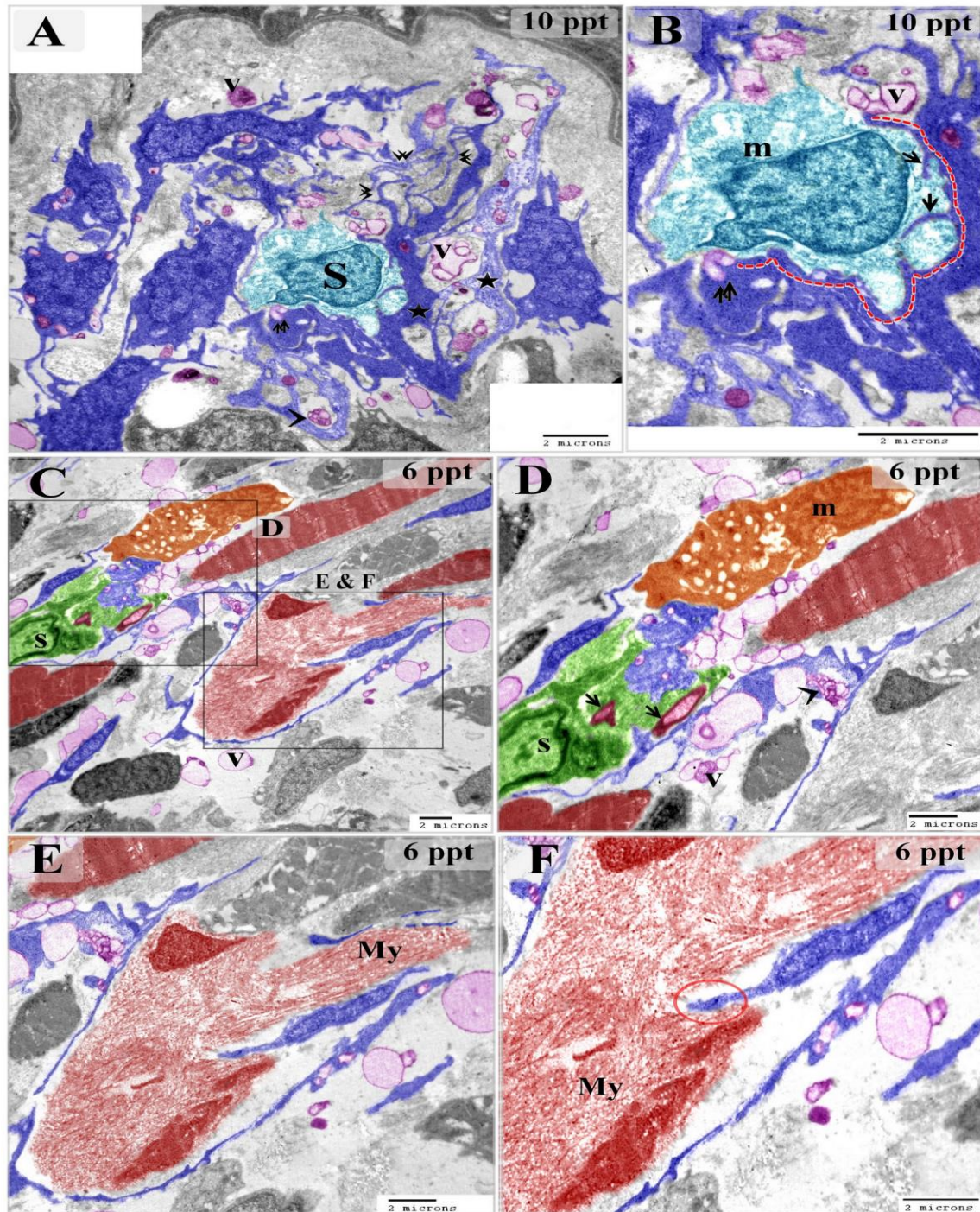


721

722 **Figure 10: changes of chloride cells in different salinity levels**

723 Colored ultra-thin sections in gill arches control (A) and treated samples with 6 ppt
724 (B), 10 ppt (C) and 14 ppt (D) level of salinity. A: chloride cell (C) appeared elongated
725 and had few oval mitochondria (arrows). B: chloride cell (C) increase in size and changed
726 the morphology and appeared more elongated. The mitochondria increased in number

727 and became elongated cigar-shaped (arrows). D: chloride cells (C) enlarged and
728 appeared cuboidal in shape. They had a large number of mitochondria; some of which
729 were elongated cigar-shaped (arrows). Note the secretory vesicles of telocytes in vicinity
730 to chloride cell. E: Chloride cell (C) hypertrophied and appeared oval-shaped. They had a
731 massive mitochondrial content. Some mitochondria were cigar-shaped (arrows). Note
732 telocytes in closed relation to chloride cell. Telopodes (double arrows). The secretory
733 vesicles (V).
734



735

736 **Figure 11: stromal telocytes relation with stem cell and skeletal myoblast.**

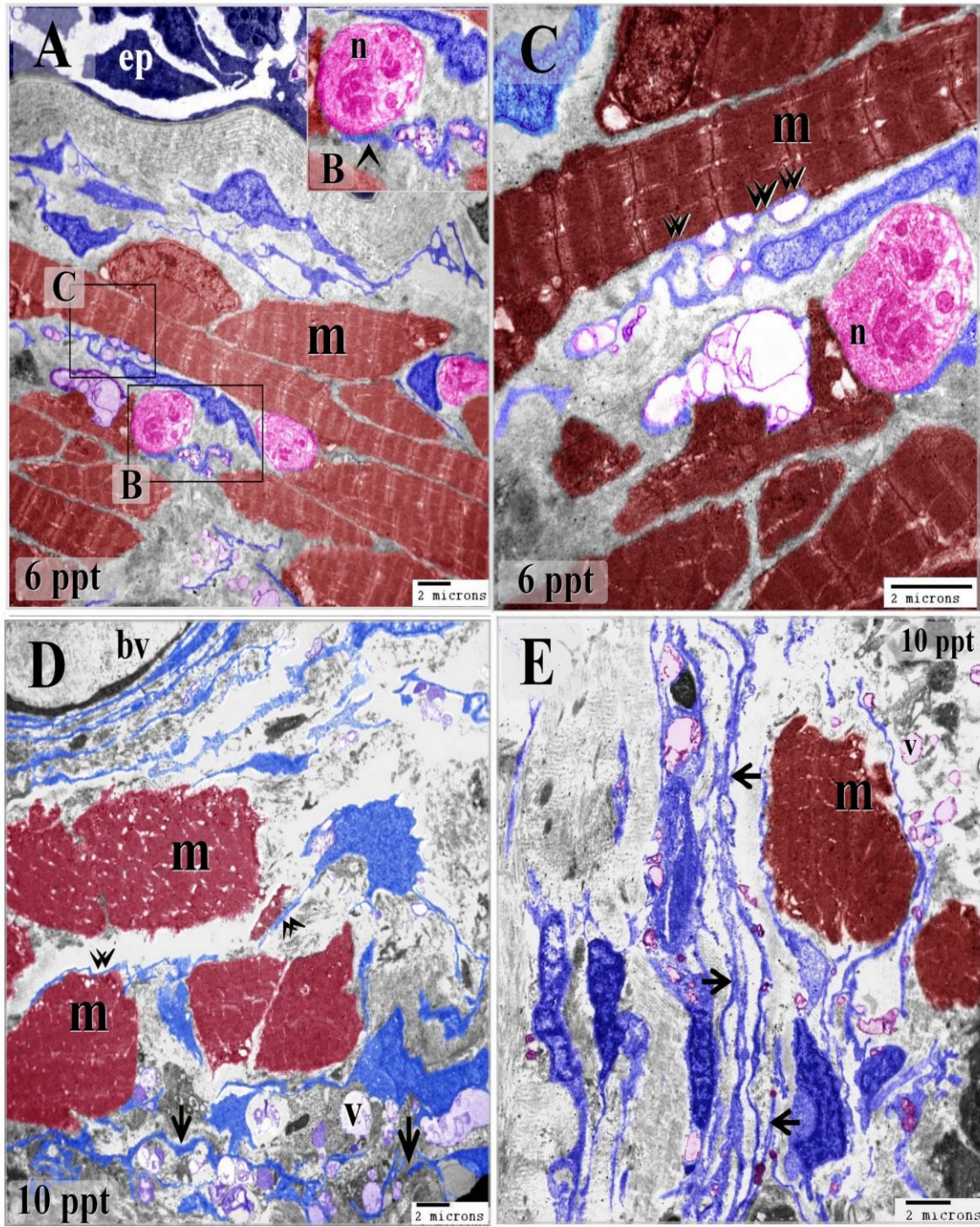
737 Colored ultra-thin sections in gill arches treated samples with 6 ppt (C-F),10 ppt (A, B)

738 level of salinity. A, B: several stromal telocytes wrapped around stem cell (S) which

739 contained mitochondria (m). telopodes established a planer contact with stem cells

740 (dashed line). telopodes formed an extensive network (double arrowheads). They secreted

741 vesicles (V), multi-vesicular body (arrowhead). Several telopodes interdigitated with the
742 stem cells (arrows). note secretory vesicles attached to stem cell (double arrow). Some
743 telopodes were thickened (asterisk). C-F: telocytes connected with Schwann cell (s) and
744 macrophage (m). note nerve fiber (arrow), secretory vesicles (V), multi-vesicular body
745 (arrowhead). Telocytes established direct contact (red circle) with myoblast which
746 contained ill-organized myofibrils (My).
747



748

749 **Figure 12: skeletal muscle fibers undergo hypertrophy in response to salinity**

750 Colored ultra-thin sections in gill arches control (A) and treated samples with 6 ppt (A-

751 C), 10 ppt (D, E) level of salinity. A, B, C: telocytes established multi-point contact

752 (double arrows) with skeletal muscle fiber (m). telopode formed a direct contact with the

753 nerve fiber (n). note epithelium (ep). D: telocytes established direct contact (double

754 arrowheads) with skeletal muscle fibers increased in diameter (m). note telopodes
755 organized an extensive network (arrows). Note blood vessel (bv), secretory vesicles (V).
756